DOI: 10.1021/cg901010v

CRYSTAL GROWTH & DESIGN Article

2010, Vol. 10
394–405

Effects of Crystal Form on Solubility and Pharmacokinetics: A Crystal Engineering Case Study of Lamotrigine

Miranda L. Cheney,[†,‡] Ning Shan,*[,†] Elisabeth R. Healey,[†] Mazen Hanna,[†] Lukasz Wojtas,[‡] Michael J. Zaworotko,*[,‡] Vasyl Sava,[#] Shijie Song,[#] and Juan R. Sanchez-Ramos[#]

[†]*Thar Pharmaceuticals Inc, 3802 Spectrum Boulevard, Suite 120, Tampa, Florida 33612,* [‡]*Department of Chemistry, University of South Florida, 4202 East Fowler Avenue, CHE205, Tampa, Florida 33620, and* [#]*Departments of Neurology and Neurosurgery, University of South Florida, College of Medicine, James A. Haley VA Hospital, Tampa, Florida 33612*

Received August 22, 2009; Revised Manuscript Received November 4, 2009

ABSTRACT: In this contribution, we describe how the supramolecular synthon approach can be used for discovery of novel crystal forms and for enhancing the relevant preclinical properties of a low solubility antiepileptic drug, lamotrigine (6-(2,3-dichlorophenyl)-1,2,4-triazine-3,5-diamine). Ten novel crystal forms are reported: lamotrigine methylparaben cocrystal form I (1:1) (**1**), lamotrigine methylparaben cocrystal form II (1:1) (**2**), lamotrigine nicotinamide cocrystal (1:1) (**3**), lamotrigine nicotinamide cocrystal monohydrate (1:1:1) (**4**), lamotrigine saccharin salt (1:1) (**5**), lamotrigine adipate salt (2:1) (**6**), lamotrigine malate salt (2:1) (**7**), lamotrigine nicotinate dimethanol solvate (1:1:2) (**8**), lamotrigine dimethanol solvate (1:2) (**9**), and lamotrigine ethanol monohydrate (1:1:1) (**10**). A selected set of the reported crystal forms were studied to determine their dissolution rate, solubility, and pharmacokinetic behavior. The solubilities were measured in aqueous media and in acidified aqueous media (pH = 1). It was observed that **5** and **2** exhibited the highest concentration in the aqueous media and acidified aqueous media, respectively. In the pharmacokinetic study, the serum concentration of lamotrigine, measured in Sprague−Dawley rats, reached the highest level after a single-dose oral administration of **5**.

1. Introduction

It is of fundamental importance for the pharmaceutical industry to understand the nature of crystal packing and its influence upon the physicochemical properties of active pharmaceutical ingredient (API) crystal forms. Indeed, crystal form screening and identification of an optimal crystal form have become an integral part of the drug development process.[1,2] Often a pharmaceutical crystal form tends to afford a high purity product with reliable reproducibility and scalability, and it is thermodynamically more stable when compared to amorphous solids. Stable crystal forms are therefore more desired by both drug developers and regulatory bodies. In addition, although crystallization has been widely studied scientifically since at least the early 19th century, this does not mean that crystallization is predictable[3] or even controllable.[4] New crystal forms are therefore likely to be patentable in their own right since they meet the primary criteria for patentability: novelty, lack of obviousness, and utility.[5] Furthermore, it has been known for over 100 years that rate of dissolution of a solid is at least partly determined by the thermodynamic solubility of a compound,[6] and it is well recognized that, if absorption is limited by solubility, solubility critically influences the bioavailability and pharmacokinetics of an API. Given that the majority of APIs fall into Biopharmaceutical Classification Scheme[7] (BCS) classification II[8] (low solubility, high permeability), the importance of API crystal form screening and selection is increasing in scope and significance. In short, the existence of multiple crystal forms of an API (e.g., salts, cocrystals, solvates, or hydrates) affords both challenges and opportunities to the pharmaceutical industry.

Pharmaceutical salts are materials formed by an ionic API and a suitable, pharmaceutically acceptable counterion.[9] They have been a part of crystal form selection for decades as they offer diversity of composition and can therefore exhibit a wide range of physicochemical properties.[10] Pharmaceutical salts have been used to enhance the solubility of poorly soluble APIs which represent approximately 40% of the drugs on the market[11] and as many as 60% of APIs in development.[12] Improving the solubility or dissolution rate of a BCS Class II API is possible via pharmaceutical salt formation.[10] For example, in the late 1950s Juncher and Raaschou[13] developed three novel salt forms of penicillin V that exhibited superior dissolution profiles in comparison to the original API. When conducting a pharmacokinetic study, it was observed that the salt form enabling the highest in vivo exposure of penicillin V was the same form that possessed the most rapid dissolution rate.

A more recently applied technique for crystal form development is pharmaceutical cocrystallization. Pharmaceutical cocrystals can be defined as multiple component crystals in which at least one component is molecular and a solid at room temperature (the cocrystal former) and forms a supramolecular synthon with a molecular or ionic API.[14] Pharmaceutical cocrystals have demonstrated that they can profoundly modify the physicochemical properties of the parent API molecule,[13−22] and at least 90 APIs have been studied in the context of cocrystallization. Often APIs that are targeted for pharmaceutical cocrystallization experience undesirable solubility and/or stability and possess multiple hydrogen bonding sites.[15] A recently published study by Bak and co-workers highlighted the ability of a series of pharmaceutical cocrystals to improve the solubility of AMG 517.[16,17] In particular, the AMG 517:sorbic acid cocrystal was studied with respect to its

*To whom correspondence should be addressed. E-mail: nshan@tharpharma.com (N.S.); xtal@usf.edu (M.J.Z.).

 Published on Web 12/03/2009

stability in vitro as well as its ability to modify the plasma concentration of AMG 517 in Sprague−Dawley rats. It was found that after oral administration of a 500 mg/kg dose of the cocrystal, the C_{max} (maximum plasma concentration) and $AUC_{0\text{-}inf}$ (area under curve) were 8 and 9 times greater, respectively, compared to oral administration of the same dose of pure API. Childs et al.[18] highlighted a cocrystal that exhibited approximately 4-fold increase in plasma concentration over the pure API after a single oral dose to dogs. A review of the literature reveals that there have been eight[17−19] pharmaceutical cocrystal case studies with pharmacokinetic details reported to date, all of which support that pharmaceutical cocrystals are a viable option to enhance the clinical performance of a poorly soluble API. The importance of hydrates and solvates in pharmaceutical development has also been recognized.[20,21] Various examples have demonstrated that the formation of hydrates and solvates can significantly alter the physicochemical properties of APIs, such as chemical stability, solubility, and dissolution rate.[22]

With this in mind, we report a study of lamotrigine (6-(2,3-dichlorophenyl)-1,2,4-triazine-3,5-diamine), a triazine drug amenable to crystal engineering design strategies that exhibits poor solubility and dissolution rate in its pure crystalline form. Lamotrigine is marketed as Lamictal by GlaxoSmithKline for oral administration as a compressed or chewable tablet. It is primarily used as an anticonvulsant drug for the treatment of epilepsy as well as in the treatment of psychiatric disorders such as bipolar disorder.[23] In particular, lamotrigine is used for the treatment of generalized seizures associated with Lennox-Gastaud syndrome,[24] and it can be used in conjunction with other antiepileptic drugs such as carbamazepine, phenytoin, phenobarbital, primidone, or valproate.[25] An additional and perhaps less common use for lamotrigine is for the treatment of neuropathic pain, cluster headaches, and migraines.[26] Lamotrigine, a white to pale cream-colored powder, exhibits a pK_a of 5.7 and a melting point of 218 °C. It is very slightly soluble in water (0.17 mg/mL at 25 °C) and slightly soluble in 0.1 M HCl (4.1 mg/mL at 25 °C).[27] Lamotrigine tablets are supplied for oral administration as 25 mg, 100 mg, 150 mg, and 200 mg tablets. Various attempts have been made to solve the use limitations of lamotrigine, such as poor solubility at the higher pH conditions. Briefly, these approaches have involved the exploration of a plethora of crystal forms,[28] including salt forms, and reduction of the particle size.[29] Recently, eight novel crystal forms of lamotrigine were reported by Galcera et al.,[30] with only two salt forms (saccharinate and DL-hemitartrate dimethylsulfoxide solvate) reaching a greater maximum aqueous solubility than pure lamotrigine. A benzoate dimethylformamide solvate,[31] hydrogen phthalate dimethylformamide solvate,[32] methanol solvate,[33] isoethoinate,[34] dimethylformamide solvate,[35] methanesulfonate,[36] and monohydrate[37] have also been reported; however, only limited solubility data are available concerning these crystal forms. To date, no polymorphic form of lamotrigine has been identified in-house or, to the best of our knowledge, reported in the literature. Some of the aforementioned crystal forms, particularly those involving certain salt forms, are undesirable for certain routes of administration, such as parenteral, due to their acidity. Other formulations contain ingredients that are not safe for human consumption such as dimethylformamide. Clearly, there is a strong scientific and clinical need to develop novel forms of lamotrigine that have significantly improved physicochemical properties, including aqueous solubility, which can be formulated for use in various delivery routes, such as oral administration.

Scheme 1. Molecular Structures of Cocrystal and Salt Formers

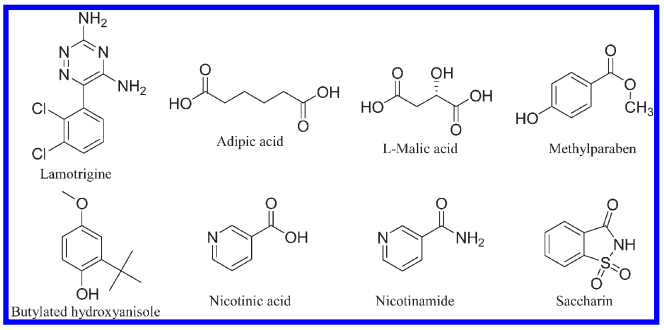

To generate novel crystal forms of lamotrigine, an analysis based upon crystal engineering,[2] molecular recognition, and supramolecular synthon formation[38,39] was conducted to determine complementarities between a number of pharmaceutically acceptable and/or approved materials containing carboxylic acid, alcohol, and primary amide moieties and lamotrigine. The ultimate goal of this approach, namely, the supramolecular synthon approach, was to effectively prioritize all possible guest molecules for crystal form screening of drugs, and to avoid the "tactless" high-throughput screening based on trial-and-error. In practice, the supramolecular synthon approach was performed by careful analysis of the Cambridge Structural Database (CSD).[40,41] It showed that lamotrigine can form complexes with two dominant supramolecular synthon motifs, with or without the aminopyridine dimer. Among all pharmaceutically acceptable and/or approved compounds with hydrogen-bonding functionality, a variety of guest molecules that were likely to form either of these two motifs with lamotrigine were selected for this study. All selected guest molecules except butylated hydroxyanisole successfully formed complexes with lamotrigine, resulting in 10 novel lamotrigine crystal forms. Details of the supramolecular synthon approach and the development of 10 crystal forms of lamotrigine from established cocrystallization techniques[39,42] are presented herein. Solubility and pharmacokinetic studies were conducted upon a subset of these crystal forms.

2. Materials and Methods

2.1. Materials. Lamotrigine was supplied by Jai Radhe Sales, India, with a purity of 99.79% and was used without further purification. All other chemicals were supplied by Sigma-Aldrich and used without further purification.

2.2. Crystal Form Synthesis. Lamotrigine was reacted with seven compounds shown in Scheme 1, namely, methylparaben, nicotinamide, saccharin, adipic acid, L-malic acid, nicotinic acid, and butylated hydroxyanisole resulting in the formation of 10 crystalline cocrystals, salts, or solvates of lamotrigine. Multiple functional groups that would facilitate the complex formation with lamotrigine have been preidentified based on the supramolecular synthon approach. Pharmaceutically acceptable and/or approved materials possessing those functional groups were awarded high priority in the selection of materials for form screening. The above seven compounds covered a variety of those high-priority materials, while each of them represented a distinct class. To date, all compounds except butylated hydroxyanisole formed complexes with lamotrigine successfully. Interestingly, attempts of complexing butylated hydroxyanisole with lamotrigine resulted in the formation of lamotrigine dimethanol solvate.

Synthesis of Lamotrigine Methylparaben Cocrystal Form I (1:1), 1. 0.0117 g (0.046 mmol) of lamotrigine and 0.0750 g (0.490 mmol)

of methylparaben were dissolved in ca. 2 mL of tetrahydrofuran (THF) and the resulting solution was left to evaporate at room temperature. Colorless crystals were afforded within seven days. **1** crystallized concomitantly with methylparaben and lamotrigine THF solvate. Single crystals of **1** were isolated from this mixture.

Synthesis of Lamotrigine Methylparaben Cocrystal Form II (1:1), 2. This cocrystal was made via multiple methods: (i) solvent-drop grinding − 0.0722 g (0.282 mmol) lamotrigine was ground with 0.0458 g (0.301 mmol) of methylparaben with 40 μL of THF for 30 min in a mechanical ball-mill with ca. 100% conversion; (ii) slurry − 0.0486 g (0.190 mmol) of lamotrigine and 0.0294 g (0.193 mmol) of methylparaben were slurried with ca. 3 mL of water at room temperature for 24 h. **2** was isolated via filtration in 70% yield; (iii) melt − 0.0751 g (0.293 mmol) of lamotrigine and 0.0485 g (0.319 mmol) of methylparaben were placed in an oven at 115 °C for 2 h. **2** was obtained via slow cooling to room temperature in 97% yield. Single crystals of X-ray diffraction quality were obtained from slow cooling of the melt.

Synthesis of Lamotrigine Nicotinamide Cocrystal (1:1), 3. This cocrystal was prepared via multiple methods: (i) solvent-drop grinding − 0.2081 g (0.813 mmol) of lamotrigine and 0.2056 g (1.68 mmol) of nicotinamide were ground with 40 μL of methanol for 30 min in a mechanical ball-mill with ca. 100% conversion; (ii) melt − 0.7105 g (2.77 mmol) of lamotrigine and 0.3496 g (2.86 mmol) of nicotinamide were heated at 125 °C for 2.5 h resulting in 98% yield; (iii) lamotrigine nicotinamide cocrystal hydrate, **4**, can be dehydrated to isolate **3** after heating at 160 °C for 6 h.

Synthesis of Lamotrigine Nicotinamide Cocrystal Monohydrate (1:1:1), 4. This cocrystal was made from two methods: (i) slurry − 0.0641 g (0.250 mmol) of lamotrigine and 0.0614 g (0.503 mmol) of nicotinamide (1:2 molar ratio) were slurried with ca. 1 mL of ethyl acetate for 24 h. The resulting solid was isolated and filtered for further use with 92% yield; (ii) solution − 0.1021 g (0.399 mmol) of lamotrigine and 0.0515 g (0.422 mmol) nicotinamide dissolved in 600 μL of *n*-butanol. The resulting solution was left to slowly evaporate at room temperature. Colorless crystals of **4** were formed within two weeks in 95% yield. The crystals were dehydrated in an oven at 160 °C for 6 h to form anhydrous cocrystal **3**.

Synthesis of Lamotrigine Saccharinate Salt (1:1), 5. This salt was made via multiple methods: (i) slurry − 50.20 g (196 mmol) lamotrigine and 35.50 g (194 mmol) of saccharin were slurried in 500 mL water overnight under ambient conditions. The solid was isolated via filtration in 83% yield. (ii) solution − 0.0102 g (0.040 mmol) of lamotrigine and 0.0103 g (0.056 mmol) of saccharin were dissolved in ca. 2 mL of methanol. The solution was left to slowly evaporate at room temperature. Colorless crystals of **5** were afforded within seven days in 94% yield.

Synthesis of Lamotrigine Adipate Salt (2:1), 6. 0.0158 g (0.062 mmol) of lamotrigine and 0.0108 g (0.074 mmol) of adipic acid were dissolved in ca. 2 mL of methanol and the resulting solution was left to slowly evaporate at room temperature. Colorless crystals of **6** appeared within seven days in 91% yield.

Synthesis of Lamotrigine Malate Salt (2:1), 7. 0.0199 g (0.078 mmol) of lamotrigine and 0.0120 g (0.089 mmol) of L-malic acid were dissolved in ca. 2 mL of methanol and the resulting solution was left to slowly evaporate at room temperature. Colorless crystals of **7** appeared within seven days in 92% yield.

Synthesis of Lamotrigine Nicotinate Dimethanol Solvate (1:1:2), 8. A solution of ca. 2 mL of methanol, 0.0148 g (0.058 mmol) of lamotrigine, and 0.0075 g (0.061 mmol) of nicotinic acid was left at room temperature to slowly evaporate. Colorless crystals of **8** formed after two days in 78% yield.

Synthesis of Lamotrigine Dimethanol Solvate (1:2), 9. 0.0213 g (0.083 mmol) of lamotrigine and 0.0148 g (0.082 mmol) of butylated hydroxyanisole were dissolved in ca. 2 mL of methanol, and the resulting solution was left to slowly evaporate at room temperature. Colorless crystals of **9** were afforded within five days in 93% yield.

Synthesis of Lamotrigine Ethanol Monohydrate (1:1:1), 10. 0.0819 g (0.320 mmol) of lamotrigine and 0.0415 g (0.340 mmol) of nicotinamide were dissolved in ca. 3 mL of a 1:1 ethanol/water solution mixture while heating followed by rapid cooling. The sample was left at room temperature and allowed to slowly evaporate. Colorless crystals of **10** were afforded within two weeks in 74% yield.

2.3. Crystal Form Characterization. Single-Crystal X-ray Diffraction. Single crystals were obtained for nine compounds. Attempts to crystallize **3** did not afford crystals suitable for single crystal X-ray crystallographic analysis. Single crystal analysis for **1**, **2**, and **5**−**10** was performed on a Bruker-AXS SMART APEX CCD diffractometer with monochromatized Mo Kα radiation (λ = 0.71073 Å) connected to a KRYO-FLEX low-temperature device while **4** was collected using Cu Kα radiation (λ = 1.54178 Å). Data for **1**, **2**, and **5**−**10** were collected at 100 K. Data for **4** was collected at 293 K. Lattice parameters were determined using the difference vector method, and reflection data were integrated using SAINT.[43] Structures were solved by direct methods and refined by full matrix least-squares based on F^2 using the SHELXTL package.[44] All nonhydrogen atoms were refined with anisotropic displacement parameters. All hydrogen atoms bonded to carbon, nitrogen, and oxygen atoms were placed geometrically and refined with an isotropic displacement parameter fixed at 1.2 times U_q of the atoms to which they were attached. Hydrogen atoms bonded to methyl groups were placed geometrically and refined with an isotropic displacement parameter fixed at 1.5 times U_q of the carbon atoms.

Powder X-ray Diffraction (PXRD). 2−**8** were characterized by a D-8 Bruker X-ray powder diffractometer using a Cu Kα radiation (λ = 1.54178 Å), 40 kV, 40 mA. Data were collected over an angular range of 3° to 40° 2θ value in continuous scan mode using a step size of 0.05° 2θ value and a scan speed of 1.0°/min. Crystal forms **1**, **9**, and **10** were not stable to loss of solvent or could not be made in sufficient quantities to collect an experimental PXRD.

Calculated PXRD. Calculated PXRD diffractograms were generated from the single crystal structures using Mercury 1.5 (Cambridge Crystallographic Data Centre, UK) for the following complexes: **1**−**2**, **4**−**10**.

Differential Scanning Calorimetry (DSC). DSC was performed on a Perkin-Elmer Diamond DSC with a typical scan range of 25−280 °C, scan rate of 10 °C/min, and nitrogen purge of ca. 30 psi.

Thermal Gravimetric Analysis (TGA). TGA analysis was performed on a Perkin-Elmer STA 6000 with a typical scan range of 30−300 °C, scan rate of 10 °C/min, and nitrogen purge of ca. 20 psi. The resulting thermograms were processed using Pyris version 9.

Fourier Transform Infrared Spectroscopy (FT-IR). FT-IR analysis was performed on a Perkin-Elmer Spectrum 100 FT-IR spectrometer equipped with a solid-state ATR accessory.

Ultraviolet/Visible Spectroscopy (UV/vis). UV/vis analysis was performed on a Perkin-Elmer Lambda 25 UV/vis spectrophotometer.

High Performance Liquid Chromatography (HPLC). Analysis was performed on an HPLC system (Perkin-Elmer Instruments LLC) comprising the following units: a series 200 Gradient Pump; a 785A UV/vis Detector; a series 200 Autosampler; an NCI 900 Network Chromatography Interface and a 600 Series Link. The system was operated by a Total Chrome Workstation. The sample holder temperature was kept at 4 °C with a flow rate of 1 mL/min. The column was a Microsorb-MV 300−5 C-18 (250 × 4.6 mm × 1/4″). The mobile phase consisted of a mixture of phosphate buffer (pH 3.0) with methanol (1/1, v/v). The phosphate buffer was prepared from 50 mmol/L Na_2HPO_3 water solution with pH-controlled HCl titration.

2.4. Dissolution Study. Dissolution studies were performed on **2**, **3**, **4**, and **5** allowing for representative crystal forms from different crystal form categories (i.e., salt, cocrystal, and solvate) to be compared against the original API. Both deionized water (25 °C) and pH 1 aqueous solution (0.1 M HCl, 37 °C) were used. The pH and temperature conditions were selected to facilitate a direct comparison to the literature and subsequent animal pharmacokinetic study. The crystal forms were sieved to achieve a particle size between 53 and 75 μm. The dissolution study was conducted using an excess of free-flowing solid in solution; that is, 100 mg of each solid was used in ca. 100 mL of water and 500 mg of each solid was used in ca. 50 mL of 0.1 M HCl. The slurries were stirred with a magnetic stir bar at a rate of ca. 200−300 rpm. Aliquots were filtered with 0.45 μm filters after 5, 10, 20, 30, 40, 50, 60, 75, 90, 105, 120, 150, 180, and 240 min. The resulting solution was processed and the concentration of lamotrigine was measured using a UV/vis spectrophotometer. The pH values of the resulting solutions and crystal forms of the solid in

Table 1. pK_a Values and the Resulting ΔpK_a Values for the Lamotrigine Salts

acid	pK_a	ΔpK_a
adipic acid	4.43	1.27
L-malic acid	3.44	2.26
nicotinic acid	4.92	0.78
saccharin	1.60	4.10

those solutions were also determined. The experiment was repeated twice to allow for statistical analysis.[45]

2.5. Animal Pharmacokinetic (PK) Study. Twenty-four hour animal PK studies were conducted using a single-dose oral administration of lamotrigine as well as **3**, **4**, and **5**. Five male Sprague−Dawley rats (225−250 g) with preimplanted indwelling jugular vein catheters were used for each crystal form. The animals were allowed water ad libitum and fasted overnight before drug administration. The crystal forms were administered via oral gavage with a dosage of 10 mg/kg lamotrigine or its equivalent, in the 1 mL suspension vehicle of a 5% PEG 400 and 95% methyl cellulose aqueous solution. All crystal forms were observed insoluble in the vehicle. After dosing, 0.2 mL of blood was withdrawn at 0, 30, 60, 120, 180, 240, 480, 720, and 1440 min. The blood samples were immediately clotted and centrifuged at room temperature to obtain the rat serum samples, which were subsequently processed and analyzed by HPLC according to the literature.[46] The PK data was processed by the Microsoft Office Excel 2003 software package.

3. Results and Discussion

3.1. Salt vs Cocrystal. Lamotrigine has the ability to form both salts and cocrystals due to its relatively basic nature (pK_a = 5.7). By selecting cocrystal formers with a range of varying acidities, the formation of lamotrigine pharmaceutical salts or cocrystals would be expected. The pK_a difference between lamotrigine and the adduct, ΔpK_a (i.e., ΔpK_a = pK_a base − pK_a acid), is widely accepted as the key to predicting whether a salt or cocrystal forms.[9,47] It is generally considered that if ΔpK_a > 3 the resulting compound will be a salt (exemplified in this study by saccharin), whereas the result is typically a cocrystal if ΔpK_a < 0. For ΔpK_a between 0 < ΔpK_a < 3 the outcome can be either a salt or cocrystal or a complex with partial proton transfer.[48] The pK_a and ΔpK_a values[49] involved in this study are summarized in Table 1. It is noted that the ΔpK_a values of three cocrystal formers (i.e., adipic acid, L-malic acid, and nicotinic acid) fall in the variable region. Interestingly, all of these cocrystal formers produce lamotrigine salts, as evidenced by the proton location and bond length analysis from the single crystal X-ray diffraction data. Analysis of the carbonyl region of the solid-state FT-IR spectrum also supports the formation of lamotrigine salts.

3.2. CSD Analysis. In order to prepare novel crystal forms of lamotrigine, a crystal engineering[2] study incorporating supramolecular design and the molecular functionality of lamotrigine, that is, the supramolecular synthon approach, was conducted. The crystal structure of pure lamotrigine exhibits two dominant supramolecular synthon motifs, the aminopyridine dimer (motif 1) and the amine−aromatic nitrogen synthon (motif 2). Motif 1 and motif 2 are depicted in Figure 1. The introduction of an additional complementary component to the crystal lattice of lamotrigine could lead to an interruption of motifs 1 or 2 by either: breaking the aminopyridine dimer (breaking motif 1) or breaking the exterior bifurcated interactions between the aromatic nitrogen moieties of one lamotrigine to the primary amine moieties of two additional lamotrigine molecules (breaking motif 2). An analysis of the CSD indicates that breaking

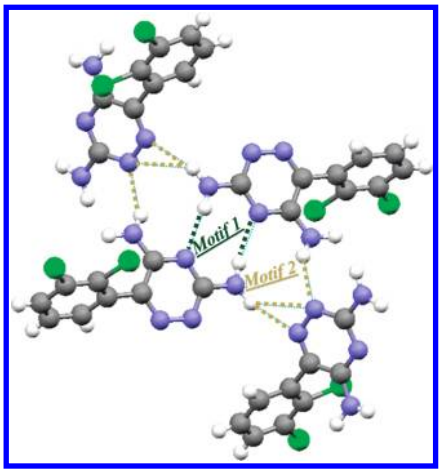

Figure 1. Motif 1 involves breaking the aminopyridine dimer and motif 2 retains the aminopyridine dimer but breaks the exterior bifurcated interaction.

either motif is feasible given a complementary secondary component. Disruption of motif 1 occurs in 26 out of 81 aminopyridine entries (32%) and disruption of motif 2 occurs in 39 out of those 81 entries, or 48% of the time. In order to understand the hydrogen bonding of the primary amine moiety of the diaminopyridine moiety, the 39 entries that break motif 2 were analyzed. Among those entries 95% (37/39) show the exterior amine moiety hydrogen bonding to the second molecule while only two entries (5%) show the exterior amine moiety hydrogen bonding to a molecule of the same kind, that is, another diaminopyridine (Refcodes: AMCQUN, GICWOF). On the basis of these CSD statistics,[41] breaking the supramolecular synthons of motif 1 and motif 2 is feasible; however, there remains a tendency toward persistence of the aminopyridine dimer (listing of the refcodes for these searches can be found in the Supporting Information).

Identification of complementary cocrystal formers for lamotrigine by statistical examination of the percentage of occurrence of supramolecular homosynthons versus supramolecular heterosynthons was also addressed via a CSD analysis.[41] Interactions between an aminopyridine moiety and carboxylic acid, primary amide, and alcohol moieties were examined in order to determine if the supramolecular heterosynthon or the supramolecular homosynthon would be more prominent (Table 2, aminopyridine was chosen instead of diaminopyridine to provide a larger data set for the statistical analysis).

To conduct the supramolecular homosynthon and heterosynthon analysis, a broad distance range was initially selected and then reduced by visual inspection to determine the appropriate ranges for defining hydrogen bond contact limits. The values given in Table 2 are a refined data set which includes only aminopyridine and one additional moiety sustained by a specified supramolecular hetero- or homosynthon interaction within a defined distance range. Our analysis concluded that, in general, the supramolecular heterosynthons were more dominant than the homosynthons. The alcohol moiety was the most statistically favored to interact with the aminopyridine moiety as there was 33% (100/307) versus 21% (66/307) occurrence for the supramolecular heterosynthon and homosynthon, respectively. There was also a preference for the aminopyridine−acid supramolecular heterosynthon, with a higher

Table 2. Comparison of Supramolecular Homosynthon versus Supramolecular Heterosynthon with Aminopyridines and Complementary Moieties

complementary moiety	no. of entries w/ both groups	% homosynthon occurrence: aminopyridine refined data set (distance range)	%homosynthon occurrence: moiety refined data set (distance range)	%heterosynthon occurrence refined data set	heterosynthon distance range (Å) refined data set
carboxylic acid	91	40/91 (44%) (N···N 2.92−3.17)	0	42/91-acid (46%) 28/91-carboxylate (31%)	N(py)···O 2.50−2.80 N(am)···O 2.71−3.10 (acid and carboxylate)
primary amide	15	2/15 (13%) (N···N 3.04−3.077)	1/15 (6%) (N···O 2.98)	1/15 (6%)	N(py)···N 2.97 N(am)···O 3.06
alcohol	307	66/307 (21%) (N···N 2.92−3.17)	78/307 (25%) (O···O2.61−2.92)	100/307 (33%)	N(py)···O 2.67−2.90 N(am)···O 2.78−3.19

percentage of occurrence attributed to the carboxylic acid group (43/91, 46%) than the carboxylate group (28/91, 31%). Interestingly, the carboxylic acid homosynthon does not occur in the presence of the aminopyridine functional group. There are 15 structures that contain aminopyridine and primary amide moieties, 2 of which form the aminopyridine supramolecular homosynthon, 1 forms the amide dimer, and 1 forms the aminopyridine−amide supramolecular heterosynthon. Unfortunately, this paucity of data precludes determination of the reliability of the aminopyridine−amide supramolecular heterosynthon. However, the CSD analysis indicates that aminopyridines are likely to form supramolecular heterosynthons with molecules containing alcohols and carboxylic acids.

3.2.1. Motif 1 versus Motif 2. The crystal forms presented herein break either motif 1 or motif 2 present in pure lamotrigine by incorporating a complementary cocrystal former. Motif 1 is broken in 4 out of 9 structures, while the remaining crystal forms contain motif 1 but break motif 2. Specifically, crystal forms **2**, **4**, **7**, **9**, and **10** break motif 2, while forms **1**, **5**, **6**, and **8** break motif 1. The individual motifs and how they impact the physicochemical properties of the crystal form are discussed in the following segments.

3.2.2. Lamotrigine Methylparaben Cocrystal Form I, 1. Cocrystals of lamotrigine methylparaben form I (**1**) crystallize in the space group $P2_1/n$ (Figure 2). The asymmetric unit contains one lamotrigine and one methylparaben molecule. The lamotrigine aminopyridine dimer is not observed in **1**. Instead, the structure is a corrugated tape sustained by two hydrogen bonds linking lamotrigine and methylparaben. Specifically, the aromatic nitrogen N2 of the triazine ring is hydrogen bonded to the hydroxyl moiety of the methylparaben [O1−H10O···N2: O···N 2.651(4) Å, H···N 1.831 Å, O−H···N 164.8°] and the amine in the 5-position of lamotrigine is hydrogen bonded to the carbonyl group of the ester moiety of methylparaben [N5−H3N···O2: N···O 2.823(4) Å, H···O 1.971 Å, N−H···O 162.7°]. The tapes are held together by various weak interactions including C−H···N and Cl···Cl interactions.

3.2.3. Lamotrigine Methylparaben Cocrystal Form II, 2. Lamotrigine methylparaben form II (**2**) can be obtained via grinding, slurry, or melt. Crystals of **2** exist in space group $P\bar{1}$ with one lamotrigine and one methylparaben in the asymmetric unit (Figure 3). The chlorinated phenyl ring backbone of lamotrigine is disordered over two distinct positions with 40% and 60% occupancies, respectively. The attached chlorine atoms are refined over three positions with occupancies of 40%, 40%, and 20%, respectively. A comparison of the crystal structures of **1** and **2** reveals that they exhibit different molecular packing arrangements. Unlike **1**, **2** exhibits lamotrigine centrosymmetric aminopyridine dimers [N3−H3B···N4: N···N 3.121(4) Å, H···N 2.246 Å, N−H···N 172.3°]. The lamotrigine dimers connect to neighboring dimers via methylparaben molecules, thereby forming supramolecular ribbons that extend parallel to the *a*-axis [N5−H5A···O1: N···O 3.036(4) Å, H···O 2.205 Å, N−H···O 157.3°; O1−H1C···N2: O···N 2.711(4) Å, H···N 1.876 Å, O−H···N 173.3°]. The methylparaben molecule also serves as a bridge to join these supramolecular ribbons via N−H···O interactions [N5−H5B···O2: N···O 2.931(4) Å, H···O 2.129 Å, N−H···O 151.2°].

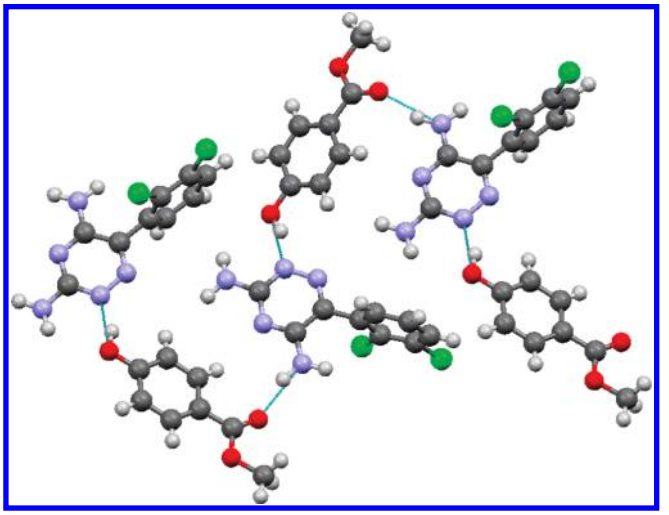

Figure 2. 1 breaks motif 1 as shown in the hydrogen bonding pattern.

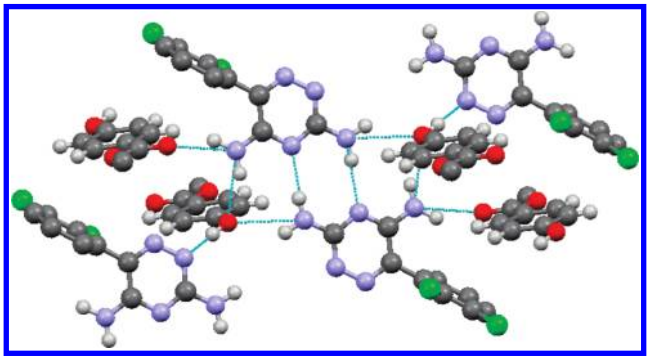

Figure 3. Breaking motif 2 shown in the hydrogen bonding of **2**; disordered molecular moieties have been omitted for clarity.

3.2.4. Lamotrigine Nicotinamide Cocrystal, 3. The cocrystal of lamotrigine and nicotinamide (**3**) was prepared from a melt of a 1:1 ratio of lamotrigine and nicotinamide, as evidenced by PXRD characterization. Because of their basic nature, both lamotrigine and nicotinamide should remain neutral in the crystal lattice of **3**. Efforts to prepare quality

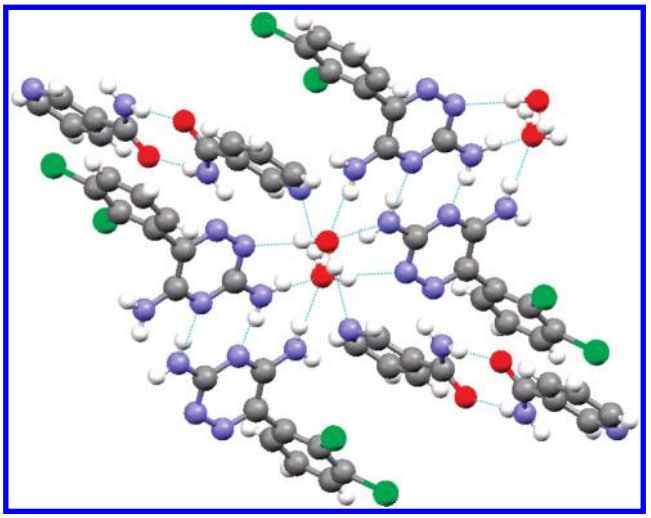

Figure 4. Hydrogen bonding of **4** interrupting motif 2.

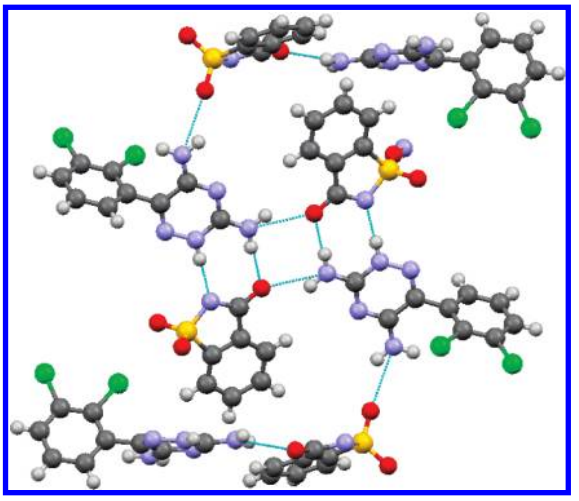

Figure 5. Hydrogen bonding of **5** interrupting motif 1.

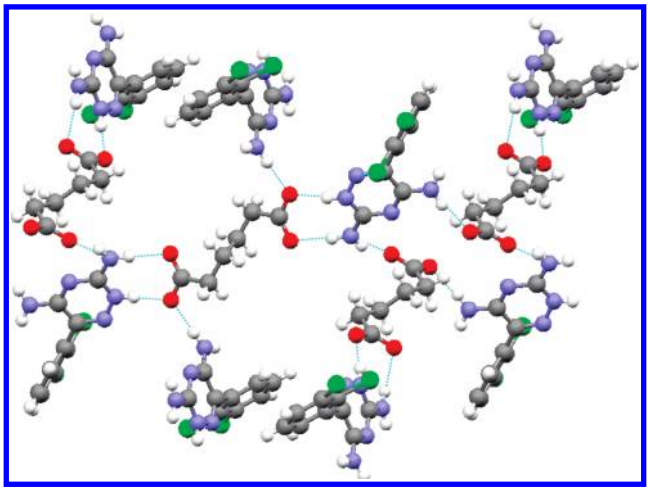

Figure 6. Hydrogen bonding in compound **6**, highlighting motif 1, breaking the aminopyridine dimer.

single crystals of **3** for single crystal XRD analysis are unsuccessful to date.

3.2.5. Lamotrigine Nicotinamide Cocrystal Monohydrate, 4. **4** crystallizes in the space group $P\bar{1}$, with the asymmetric unit consisting of one molecule of lamotrigine, one molecule of nicotinamide, and one water molecule (Figure 4). Lamotrigine molecules form aminopyridine dimers [N3−H2N···N4: N···N 3.039(2) Å, H···N 2.243 Å, N−H···N 154.2°]. Supramolecular ribbon motifs are formed along the *b*-axis as the lamotrigine dimers are linked by water molecules via N−H···O and O−H···N interactions [N5−H3N···O1−H5O···N2: N···O 2.930(2) Å, H···O 2.089 Å, N−H···O 165.3°, O···N 2.822(2) Å, H···N 1.967 Å, O−H···N 171.7°]. In addition, nicotinamide molecules form centrosymmetric amide dimers that pack in the layers between the ribbons of lamotrigine supramolecular units [N7−H8N···O2: N···O 2.915(3) Å, H···O 2.056 Å, N−H···O 176.7°]. The water molecules within the ribbons hydrogen bond to nicotinamide dimers via additional O−H···N interactions [O1−H6···N6: O···N 3.039(3) Å, H···N 2.162 Å, O−H···N 166.5°]. By heating **4** at 160 °C for 6 h, it desolvated and converted to **3**.

3.2.6. Lamotrigine Saccharinate Salt, 5. The salt of lamotrigine and saccharin (**5**) crystallizes in space group $P2_1/c$. The asymmetric unit contains one lamotrigine cation and one saccharin anion. The structure of **5** does not contain the aminopyridine dimer; however, formation of the dimer is possible with protonation of the most basic nitrogen (N2) as it is not incorporated in the lamotrigine dimer. The basic supramolecular unit in **5** is a tetramer formed between two lamotrigine and two saccharin ions where N2 is protonated (Figure 5). Lamotrigine and saccharin are associated via two 2-point recognition aminopyridine-sulfonamide supramolecular heterosynthons [$N2^+$−H1N···N6: N···N 2.819(2) Å, H···N 1.940 Å, N^+−H···N 177.5°; N3−H2N···O1: N···O 2.830(2) Å, H···O 1.954 Å, N−H···O 173.5°]. The C3−N2−N1 angle of the triazine ring in the crystal structure of **5** is 123.4° which correlates to the previously reported values for protonated lamotrigine[50] and the expected trend for protonated aminopyridines, that is, higher angles than those of a neutral aminopyridine.[50,51] The tetramer is formed from two adjacent supramolecular heterosynthon dimers that are further connected by primary amine−carbonyl interactions [N3−H3N···O1: N···O 2.818(2) Å, H···O 2.054 Å, N−H···O 144.7°]. Each tetramer is hydrogen bonded to four additional tetramers via either sulfonyl-amine or sulfonyl−chlorine interactions [N5−H4N···O2: N···O 2.889(2) Å, H···O 2.194 Å, N−H···O 135.5°; Cl1···O3 3.068(3) Å].

3.2.7. Lamotrigine Adipate Salt, 6. **6** crystallizes in space group of $P2_1/c$ with two lamotrigine cations and one adipate dianion in the asymmetric unit. The molecular packing of **6** (Figure 6) is based upon 2-point supramolecular heterosynthons between the aminopyridinium and carboxylate moieties, involving an N−H···O hydrogen bond [N3−H3N···O1: N···O 2.942(2) Å, H···O 2.110 Å, N−H···O 157.5°] and an N^+−H···O^- charge-assisted hydrogen bond [$N2^+$−H1N···$O2^-$: N···O 2.627(2) Å, H···O 1.790 Å, N−H···O 158.1°]. Proton transfer is evidenced by the C−O bond distances of the carboxylate group (1.248(2) and 1.272(2) Å) and the geometry of the lamotrigine triazine ring. The C3−N2−N1 angle of the triazine ring in the crystal structure of **6** is 122.4(2)°. Each discrete unit, comprised of two lamotrigine cations and one adipate dianion, is hydrogen bonded to eight nearby lamotrigine-adipate units through the lamotrigine NH_2 moieties and neighboring carboxylate [N3−H2N···O1: N···O 2.861(2) Å, H···O 2.057 Å, N−H···O 151.5°;

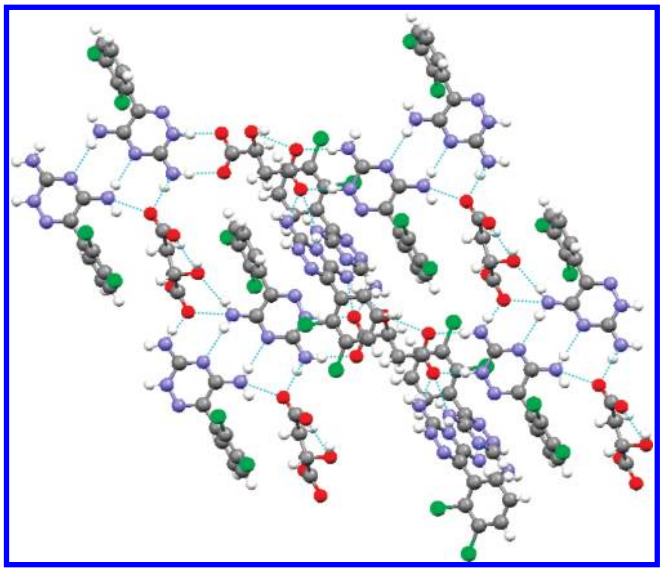

Figure 7. Hydrogen bonding of **7** breaks motif 2.

N5−H4N···O2: N···O 2.760(2) Å, H···O 1.931 Å, N−H···O 156.5°]. Each adipate dianion is hydrogen bonded to four additional discrete units via C−O···H−N interactions. The overall packing can be viewed as staggered supramolecular units of lamotrigine-adipate running parallel to either (010) or (001) with Cl···pi interactions.

3.2.8. Lamotrigine Malate Salt, 7. The salt formed by lamotrigine and L-malic acid (**7**) crystallizes in $P2_1/c$. The asymmetric unit is comprised of two lamotrigine cations and one L-malate dianion. Lamotrigine dimers are formed via a noncentrosymmetric dimer sustained by N−H···N hydrogen bonds [N5−HN5A···N14: N···N 2.956(6) Å, H···N 2.078 Å, N−H···N 174.6°; N15−H15A···N4: N···N 3.082(6) Å, H···N 2.215 Å, N−H···N 168.6°]. The L-malate dianion hydrogen bonds to the lamotrigine dimer such that a supramolecular chain is formed (Figure 7). Proton transfer occurs between both carboxylate groups (C20−O1: 1.275(5) Å; C20−O2: 1.235(6) Å; C23−O4: 1.257(6) Å; C23−O5: 1.275(6) Å); of L-malate and aromatic nitrogen atoms of lamotrigine [$N12^+$−HN12···$O1^-$: N···O 2.632(5) Å, H···O 1.766 Å, N−H···O 167.8°; C19−N12−N11 angle 123.2°]. The lengths of the C−O bonds are typical of a carboxylate moiety and the C19−N12−N11 angle of 123.2° is consistent with that of a protonated aromatic nitrogen. The supramolecular chains that are generated from two lamotrigine cations alternating with one L-malate dianion extend perpendicular to the *bc*-plane. The chains interact via NH···O hydrogen bonds [N3-HN3A···O1: N···O 2.790(5) Å, H···O 2.086 Å, N−H···O 136.3°; N13−H13A···O5: N···O 2.928(5) Å, H···O 2.135 Å, N−H···O 149.6°] to chains that run through the *ac*-plane, thereby generating a 3D structure.

3.2.9. Lamotrigine Nicotinate Dimethanol Solvate, 8. The methanol solvate of the salt formed by lamotrigine and nicotinic acid (**8**) crystallizes in space group $P2_1/c$ (Figure 8) with proton transfer observed from the carboxylic acid group to N2 on the triazine ring [$N2^+$−H1N···$O2^-$: N···O 2.729(3) Å, H···O 1.880 Å, N−H···O 161.7°; C3−N2−N1 angle 122.8°]. The structure of **8** reveals that the nicotinate anion breaks the lamotrigine dimer. Similarly to **5**, two pairs of lamotrigine nicotinate adducts interact to form tetrameric motifs sustained by charge assisted N^+−H···O^- and

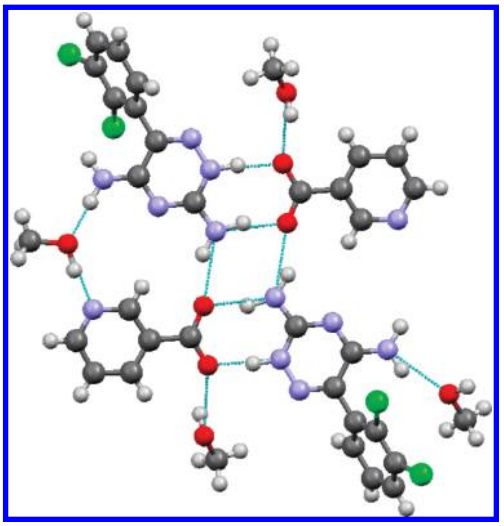

Figure 8. Breaking motif 1 shown in the hydrogen bonded assembly of **8**.

N−H···O hydrogen bonds [N3−H2N···O3: N···O 2.764(3) Å, H···O 1.9223 Å, N−H···O 159.4°, N3−H3N···O3: N···O 2.872(3) Å H···O 2.061 Å N−H···O 152.8°]. In addition, four methanol molecules attach to each tetramer by hydrogen bonding to lamotrigine cations and nicotinate anions. Two methanol molecules interact with carboxylate groups via O−H···O hydrogen bonds [O1S−H6S···O2: O···O 2.777(2) Å, H···O 1.974 Å, O−H···O 159.7°], while the other two methanol molecules are inserted between N5 and the aromatic nitrogen of nicotinate [N5−H4N···O4S: N···O 2.755(3) Å, H···O 1.881 Å, N−H···O 171.8°, O4S−H7S···N6: O−···N 2.699(3) Å, H···N 1.863 Å, O···N 172.7°].

3.2.10. Lamotrigine Dimethanol Solvate, 9. The crystal structure of lamotrigine monomethanol solvate has previously been reported.[33] In the structure of the monomethanol solvate, the basic supramolecular unit is comprised of a lamotrigine dimer with the adjacent methanol molecule hydrogen bonded to the exterior. A lamotrigine dimethanol solvate (**9**) was obtained from an attempted cocrystallization of lamotrigine and butylated hydroxyanisole from methanol. **9** crystallizes in $C2/c$ with the asymmetric unit comprised of one lamotrigine and two methanol molecules (Figure 9). **9** retains the lamotrigine dimer motif and the supramolecular unit consists of one lamotrigine dimer and two separately hydrogen bonded methanol molecules. The lamotrigine supramolecular homosynthon dimer in **9** is centrosymmetric [N3−H1N···N4: N···N 3.059(2) Å, H···N 2.189 Å, N−H···N 170.0°]. In addition, N3 and N5 amines form hydrogen bonds with methanol molecules [N3−H2N···O2: N···O 2.824(2) Å, H···O 2.210 Å, N−H···O 126.6°; N5−H3N···O2: N···O 2.862(2) Å, H···O 2.109 Å, N−H···O 143.1°]. Hydrogen bonds are also observed between methanol molecules and aromatic nitrogen atoms N1 and N2 [O1−H6O···N1: N···O 2.987(2) Å, H···N 2.159 Å, N−H···O 168.6°; O2−H5O···N2: N···O 2.654(2) Å, H···N 1.824 Å, N−H···O 169.9°]. The lamotrigine dimers and methanol molecules hydrogen bond to form a ribbon that extends along the *c*-axis. Two inversion center related ribbons interact via CH−N and Cl−pi interactions thus forming a ribbon bilayer. The bilayers stack along the *b*-axis in an *abab* motif.

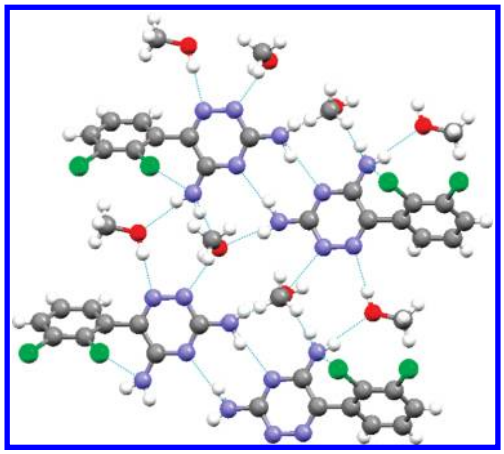

Figure 9. Crystal form **9** breaking motif 2.

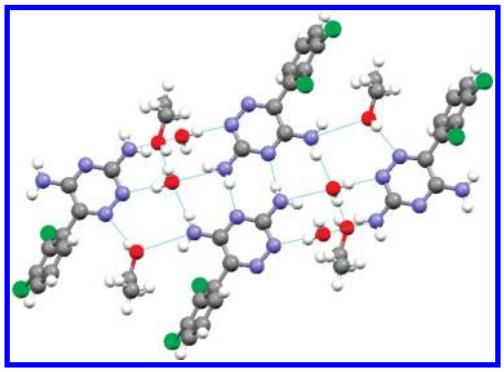

Figure 10. Crystal form **10** interrupting motif 2.

3.2.11. Lamotrigine Ethanol Monohydrate, 10. Crystals of **10** form in space group $P2_1/c$ with an asymmetric unit that is comprised of one lamotrigine, one ethanol, and one water molecule. **10** exhibits the lamotrigine dimer as shown in Figure 10. In the crystal structure of **10**, the basic supramolecular unit is the lamotrigine aminopyridine dimer sustained by two symmetrically related hydrogen bonds [N3−H2N···N4: N···N 3.006(2) Å, H···N 2.191 Å, N−H···N 153.7°]. These lamotrigine dimers are further hydrogen bonded via water molecules [N3−H1N···O1: N···O 2.928(2) Å, H···O 2.295 Å, N−H···O 128.8°; N5−H3N···O1: N···O 2.848(2) Å, H···O 1.973 Å, N−H···O 173.2°] and ethanol molecules [N5−H4N···O2: N···O 3.042(2) Å, H···O 2.346 Å, N−H···O 136.2°] to form a supramolecular ribbon parallel to the *b*-axis. Adjacent supramolecular ribbons are connected through hydrogen bonds that occur between water and ethanol molecules [O1−H9O···O2: O···O 2.829(2) Å, H···O 1.942 Å, O−H···O 178.8°], thereby generating a stacked motif. The supramolecular synthons involved in the structure of **10** are reminiscent of pure lamotrigine; however, the water and ethanol molecules force neighboring lamotrigine dimers further apart.

3.3. Solubility and Dissolution Study. As shown in Figures 11 and 12, solubility and dissolution studies were conducted for **2**, **3**, **4**, **5** and pure lamotrigine. The solubility of **5** has been reported elsewhere[30] and is re-examined in this study. The maximum concentration of pure lamotrigine in water and pH 1 HCl solution differs by approximately 10% with the higher solubility of lamotrigine exhibited under more acidic conditions. The dissolution study in water revealed

Table 3. Crystallographic Data and Structure Refinement Parameters for Compounds 1−2, 4−10

	1	**2**	**4**	**5**	**6**	**7**	**8**	**9**	**10**
chemical formula	$C_9H_7Cl_2N_5\cdot C_8H_8O_3$	$C_9H_7Cl_2N_5\cdot C_8H_8O_3$	$C_9H_7Cl_2N_5\cdot C_6H_6N_2O\cdot H_2O$	$C_9H_8Cl_2N_5\cdot C_7H_5NO_3S$	$C_9H_8Cl_2N_5\cdot (C_6H_9O_4)_{0.5}$	$(C_9H_8Cl_2N_5)_2\cdot C_4H_5O_5$	$C_9H_8Cl_2N_5\cdot C_6H_4\text{-}NO_2\cdot (CH_4O)_2$	$C_9H_7Cl_2N_5\cdot (CH_3OH)_2$	$C_9H_7Cl_2N_5\cdot C_2H_5OH\cdot H_2O$
formula weight	408.24	408.24	396.24	439.28	329.17	646.28	443.29	320.18	320.18
crystal system	monoclinic	triclinic	triclinic	monoclinic	monoclinic	monoclinic	monoclinic	monoclinic	monoclinic
space group	$P2_1/n$	$P\bar{1}$	$P\bar{1}$	$P2_1/c$	$P2_1/c$	$P2_1$	$P2_1/c$	$C2/c$	$P2_1/c$
a (Å)	5.2729(9)	8.8957(18)	7.3047(6)	18.447(5)	13.068(3)	10.728(2)	7.648(3)	19.326(4)	7.1308(14)
b (Å)	14.330(3)	11.409(2)	8.4939(7)	6.954(2)	7.498(2)	10.2003(19)	15.863(6)	17.584(3)	8.3566(16)
c (Å)	23.822(4)	12.040(2)	14.6964(12)	14.762(4)	14.069(3)	12.721(2)	16.803(7)	8.2698(15)	24.018(5)
α (°)	90	107.05(3)	105.081(5)	90	90.00	90	90	90	90
β (°)	92.795(3)	102.10(3)	90.580(5)	107.978(4)	96.755(4)	107.634(13)	90.072(6)	97.820(3)	94.565(3)
γ (°)	90	112.50(3)	95.244(5)	90	90.00	90	90	90	90
vol (Å^3)	1797.9(6)	1005.0(4)	876.21(12)	1801.2(9)	1369.0(6)	1326.6(4)	2038.5(15)	2784.2(9)	1426.7(5)
D_{cal} (g cm^{-3})	1.508	1.349	1.502	1.620	1.597	1.618	1.444	1.528	1.491
Z	4	2	2	4	4	2	4	8	4
reflections collected	8611	4879	7400	9108	6576	9647	10331	5746	8317
independent reflection	3159	3370	2842	3273	2407	3848	3642	2421	3273
observed reflection	2056	2420	2406	3033	2230	3499	2698	2127	2886
T (K)	100	100	296	100	100	100	100	100	100
R_1	0.0626	0.0642	0.0352	0.0338	0.0317	0.0461	0.0419	0.0341	0.0367
wR_2	0.1002	0.1380	0.0920	0.0893	0.0894	0.1271	0.0938	0.0889	0.0917
GOF	1.095	1.070	1.024	1.043	1.040	1.097	1.021	1.054	1.022

that **5** reached a maximum concentration of ca. 0.45 mg/mL. This observation is in agreement with the reported literature aqueous solubility.[52] However, given that the solubility of lamotrigine increased under more acidic conditions, the improved solubility of **5** in water might be rationalized by the inadvertent decrease in pH from 5.5 to 5.1. Interestingly, **5** was the only crystal form to decrease the pH value of the solution during the water dissolution study. The maximum concentrations of the other crystal forms in water were ca. 0.21 mg/mL, 0.30 mg/mL, 0.23 mg/mL, and 0.28 mg/mL for **2**, **3**, **4**, and pure lamotrigine, respectively. It was also found that **4** exhibited the lowest concentration in water after 4 h, which is not surprising as hydrates are typically considered to be less soluble than the corresponding anhydrate.[21,53] The remaining solid phase after the dissolution study was characterized by PXRD analysis. It was observed that **2** and **5** retained their respective crystal forms after the water dissolution study, while **3** and **4** converted to a hydrated form of lamotrigine.

An examination of the dissolution profiles generated at pH 1 indicates that **2** sustains the highest concentration throughout the 4-h study achieving a maximum concentration of ca. 3.8 mg/mL. **4**, however, also reaches a maximum concentration of ca. 3.8 mg/mL after only 5 min, but it then proceeds to decline over the remainder of the study. This particular type of profile is a product of the "spring and parachute effect" and has been exhibited by a number of pharmaceutical cocrystals reported recently.[16,18,54] This profile is significant because it shows that a greater concentration of API can be achieved at a much faster rate depending upon the crystal form. A similar trend is also exhibited by **4** under aqueous conditions; however, the maximum concentration of **4** was less than that of pure lamotrigine. A slurry of **3**, stirred for 5 min in acidic media, achieved a concentration ca. 36% greater than pure lamotrigine. Interestingly, **5**, which exhibits the highest concentration in aqueous solution, achieves the lowest concentration in acidic media (1.3 mg/mL). The pH values of the resulting solutions after the 0.1 M HCl slurry for **2**, **3**, **4**, **5**, and pure lamotrigine were also measured, but no significant pH change was observed. Therefore, the dissolution profiles of the acidic slurry were not affected by the pH change, even though pH 1 buffer was not used. All remaining solids converted to the lamotrigine hydrochloride salt after slurry, as evidenced by PXRD analysis. It is noted that such conversions are concomitant with the crystallization of methylparaben and saccharin during the acidic slurry of **2** and **5**, respectively. More detailed results of the dissolution study are available in the Supporting Information.

A recently published article suggests that the solubility of the cocrystal is directly proportional to the solubility of its components;[55] more specifically, the solubility ratio plotted against the solubility of the cocrystal former divided by the solubility of the API should result in a linear relationship. A similar analysis of crystal forms **2**–**5** reported herein, however, does not generate a linear plot. In fact, within this set of case studies, no clear correlation exists with respect to the solubility of the salt/cocrystal former and the solubility of the resulting crystal form. The aqueous solubility of nicotinamide is ca. 1 g/mL, the highest of all cocrystal formers studied (methylparaben = 1 g/400 mL and saccharin = 1 g/290 mL), and it is also a hydrotrope that is frequently used for solubility improvement;[56] however, the crystal forms

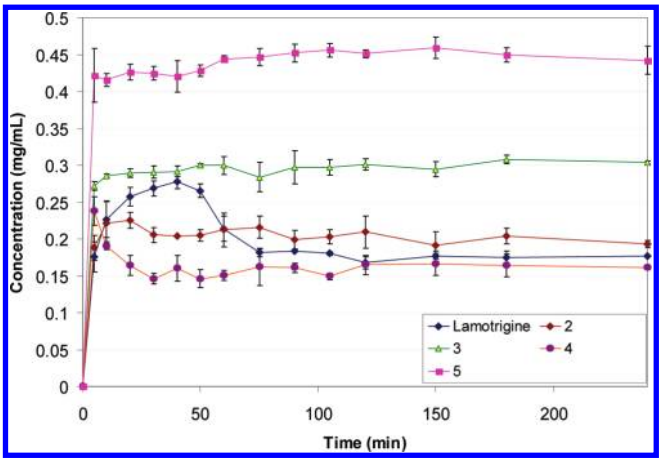

Figure 11. Dissolution profiles in water for lamotrigine and crystal forms **2**–**5**.

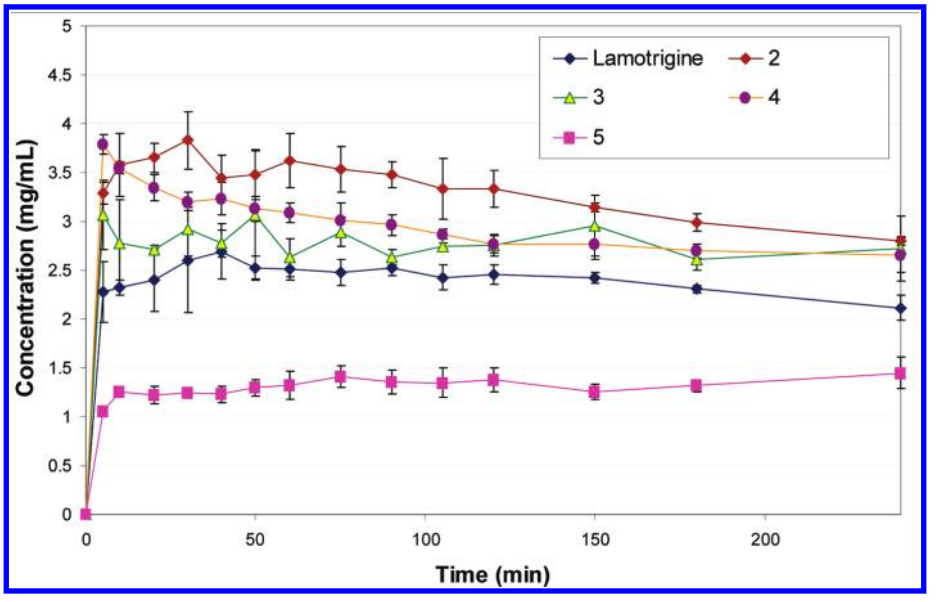

Figure 12. Dissolution profiles at pH = 1 for lamotrigine and crystal forms **2**–**5**.

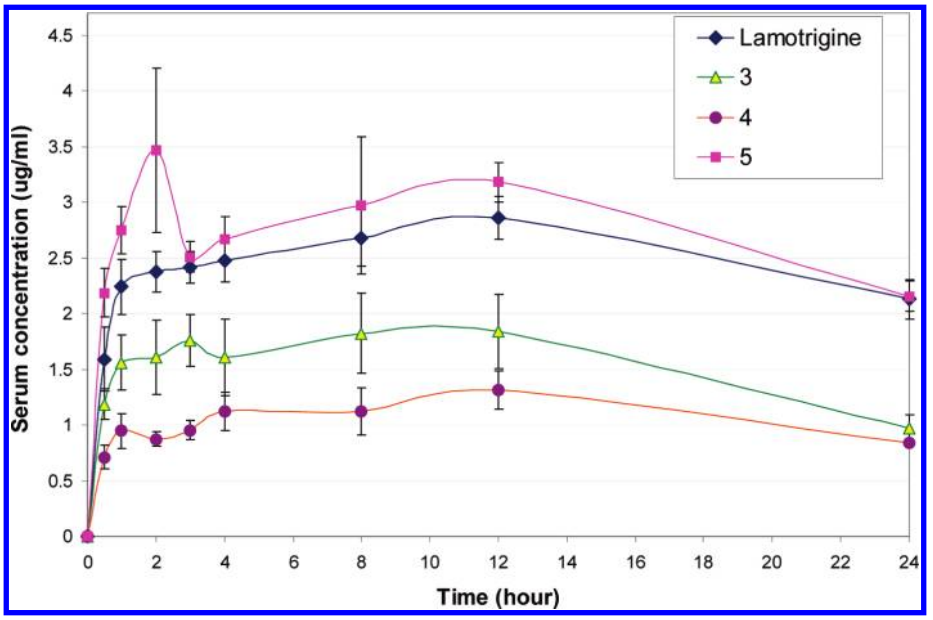

Figure 13. Rat serum concentrations of lamotrigine, **3**, **4**, and **5**.

containing nicotinamide (**3** and **4**) are not the most soluble in aqueous solutions. Instead, **5** is the most soluble crystal form most likely due to the acidic saccharin molecule altering the pH of the solution to favor the dissolution of lamotrigine. The low correlations may be due to the small data set or the inclusion of both protonated and unprotonated species in the data set.

Correlations between solubility and crystal packing were also investigated. **5**, which breaks motif 1, achieved a greater concentration in water than under acidic conditions (pH = 1). **2** and **4**, which break motif 2, show markedly improved concentrations in the acidic solution (pH = 1) but exhibited much lower concentrations in water. On the basis of this data set, it can be concluded that, for this particular case study, lamotrigine cocrystals that break motif 2 are more soluble than pure lamotrigine under acidic conditions (pH = 1), while lamotrigine salts that break motif 1 are more soluble than pure lamotrigine in aqueous solutions. However, the enhanced aqueous solubility of **5** may be attributed to the inherent acidity of saccharin.

3.4. Animal Pharmacokinetic (PK) Study. The serum concentration of lamotrigine that resulted from single-dose oral gavage of **3**, **4**, **5**, and pure lamotrigine was measured in Sprague−Dawley rats over a 24-h time period (Figure 13). **2** was not studied due to its instability after 3 months of aging at 40 °C in variable humidity. An examination of the serum concentrations after dosing with **3**, **4**, and **5** shows that the PK profile can be substantially altered via cocrystal or salt formation. Two hours after dosing the average serum concentration of **5** was 3.5 μg/mL, which is ca. 1.5 times the level shown for pure lamotrigine (2.3 μg/mL). **3** and **4** showed a decrease in the serum concentration by ca. 40% and 68%, respectively, compared to the pure lamotrigine. The area under the curve (AUC_{0-24h}) for **3**, **4**, **5** and pure lamotrigine was calculated to be 37, 26, 66, and 60 μg/mL, respectively. A comparison of the average serum concentrations showed that **5** exhibited the highest initial serum concentration, the lowest T_{max} (time to reach maximum serum concentration) and the greatest AUC_{0-24h}. Thus, **5** allowed the faster and higher absorption of lamotrigine in the gastrointestinal tract of rats. Given the increase of absorption in rats, the time required to reach the therapeutic concentration in humans could be decreased. It is possible that **5** could enable faster onset and a better clinical performance. The result of this preliminary PK study showed that **5** would be the desired crystal form for further pharmaceutical development.

An analysis of the serum concentrations for **3**, **4**, and **5** in the rat in terms of crystal packing concluded that **5**, which broke motif 1, experienced an initial boost in serum concentration of lamotrigine. Meanwhile, serum levels for cocrystals **3** and **4**, which retained the aminopyridine dimer and broke motif 2, were an average of ca. 54% less than that of pure lamotrigine, thus suggesting that crystal forms that break motif 1 could exhibit higher serum concentrations than forms that break motif 2. Interestingly, the greatest improvements in the PK study and the dissolution study occur when the aminopyridine dimer is broken. This case study also illustrates that pharmaceutical cocrystals and salts can have a significant impact upon drug development as they can greatly alter the PK profile of the parent drugs.

4. Conclusions

In summary, the work presented herein exemplifies how salt or cocrystal formers can generate novel crystalline forms of preexisting APIs with different physicochemical properties. Lamotrigine was targeted for crystal form development with the goal of improving its solubility and clinical performance. Ten crystal forms of lamotrigine were developed via the supramolecular synthon approach. The new crystal forms differed from pure lamotrigine in that either supramolecular synthon motif 1 (the aminopyridine dimer) or motif 2 (the amine-aromatic nitrogen hydrogen bond) were broken. Motif 2 was broken in 5 out of 10 structures (50%), while 4 out of 10 structures (40%) broke motif 1. Interestingly, the majority of the crystal forms that did not contain motif 1, with the exception of **1**, were all lamotrigine salts.

Several crystal forms were tested to determine solubility, dissolution rate, and rat PK profiles. Out of 10 crystal forms, four (**2**, **3**, **4**, and **5**) were selected for dissolution studies and three (**3**, **4**, and **5**) were selected for PK studies. The solubility/dissolution study was conducted under aqueous conditions

and under acidified (pH = 1) aqueous conditions. The dissolution profiles for **2** and **4** achieved concentration levels similar to lamotrigine in aqueous media, while **3** maintained a concentration equivalent to the maximum solubility of lamotrigine. The average concentrations achieved from **2**, **3**, **4**, and **5** during dissolution measurements from the acidic media surpassed the levels of pure lamotrigine by ca. 48%, 19%, 18%, and 58%, respectively. In the rat PK study, the serum concentrations for **3** and **4** were less than pure lamotrigine by 37% and 26%, respectively. **5**, however, exhibited an initial increase in the serum concentration of ca. 66%. After approximately 3 h, the serum concentration of **5** reduced to a level similar to that of pure lamotrigine.

The influence of a particular cocrystal former upon solubility and rat PK was examined. The analysis compared the solubility of the cocrystal former with the solubility and serum concentration of the subsequent crystal form. For this data set, the most soluble cocrystal former did not lead to the most soluble crystal form. In addition, a comparison of the rat PK data to the solubility of the crystal forms revealed that the crystal forms which achieved the greatest aqueous solubility also reached the highest concentrations in the rat PK data. In contrast, the solubility of the crystal form in the acidic solution did not correspond to the PK data. A further analysis showed that, except for **5**, the T_{max} for lamotrigine, **3** and **4** (10−12 h) were significantly longer than the time required for the equilibrium of solutions in the dissolution studies. This discrepancy could be rationalized by the fact that serum concentrations of all crystal forms reached ca. 90% C_{max} within 60 min, which correlated to the dissolution profiles. The slow increase of serum concentration after 60 min could be the results of the prolonged absorption of the drug in the gastrointestinal tract as well as slow metabolism and excretion.

The influence of supramolecular synthon motif upon solubility and PK was also examined. Of the crystal forms where the solubility and rat PK were measured (**3**, **4**, **5**) the only crystal form that broke the aminopyridine dimer (**5**) also achieved the highest concentration in aqueous solution and rat serum, suggesting that breaking the lamotrigine aminopyridine dimer can lead to crystal forms with desirable physicochemical properties. Therefore, when considering both aqueous dissolution and animal PK data of the crystal forms presented herein collectively, **5** exhibited the targeted physicochemical properties with substantial improvements, and would be an appropriate candidate for further development. Given the promising results of **5** shown in this study, it must be noted that the successful development of a novel crystal form of lamotrigine encompasses many factors above and beyond solubility study and rat PK study. For example, the crystal form must be proven physically stable during the accelerated stress testing and downstream processing. In addition, the crystal form has to be scaled up and further evaluated by studies including additional PK study using larger animals, animal toxicity study, and animal efficacy study. All of the above considerations will be taken into account in the planning and implementation of the future development of **5**.

Acknowledgment. We thank Mr. Raymond Houck for stimulating discussions and valuable input to the project.

Supporting Information Available: Characterization results of lamotrigine crystal forms, refcodes from the CSD statistical analysis, and more detailed experimental results of dissolution study. This information is available free of charge via the Internet at http://pubs.acs.org/.

References

(1) (a) Gardner, C. R.; Walsh, C. T.; Almarsson, Ö. *Nat. Rev. Drug Discovery* **2004**, *3*, 926. (b) Vishweshwar, Peddy; McMahon, J. A.; Bis, J. A.; Zaworotko, M. J. *J. Pharm. Sci.* **2006**, *95*, 499. (c) Allen, L. V.; Popovich, N. G.; Ansel, H. C. *Ansel's Pharmaceutical Dosage Forms and Drug Delivery Systems*, 8th ed.; Lippincott Williams and Wilkins: New York, 2005; (d) Blagden, N.; de Matas, M.; Gavan, P. T.; York, P. *Adv. Drug Delivery Rev.* **2007**, *59*, 617.
(2) (a) Desiraju, G. R. *Crystal Engineering: The Design of Organic Solids*; Elsevier: New York, 1989; (b) Pepinsky, R. *Phys. Rev.* **1955**, *100*, 971. (c) Schmidt, G. M. J. *Pure Appl. Chem.* **1971**, *27*, 647.
(3) Maddox, J. *Nature* **1988**, *335*, 201. Ball, P. *Nature* **1996**, *381*, 648.
(4) Dunitz, J. D.; Bernstein, J. *Acc. Chem. Res.* **1995**, *28*, 193.
(5) Trask, A. V. *Mol. Pharmaceutics* **2007**, *4*, 301.
(6) Noyes, A. A.; Whitney, W. R. *J. Am. Chem. Soc.* **1897**, *19*, 930.
(7) Takagi, T.; Ramachandran, C.; Bermejo, M.; Yamashita, S.; Yu, L. X.; Amidon, G. L. *Mol. Pharmaceutics* **2006**, *3*, 631.
(8) Hiten, J. S.; Gunta, S.; Dasharath, M. P.; Chhagan, N. P. *Biopharm. Drug Dispos.* **2009**, *30*, 524−531.
(9) Stahl, P. H.; Wermuth, C. G. *Handbook of Pharmaceutical Salts: Properties, Selection, and Use*; WILEY-VCH: Zurich, 2002.
(10) Berge, S. M.; Bighley, L. D.; Monkhouse, D. C. *J. Pharm. Sci.* **1977**, *66*, 1.
(11) Lipinski, C. A. *Am. Pharm. Rev.* **2002**, *5*, 82.
(12) Dublin, C. H. *Drug Delivery Technol.* **2006**, *6*, 34.
(13) Juncher, H.; Raaschou, F. *Antibiot. Med. Clin. Ther.* **1957**, *4*, 497.
(14) (a) Almarsson, Ö.; Zaworotko, M. J. *Chem. Commun.* **2004**, 1889. (b) Shan, N.; Zaworotko, M. J. *Drug Disc. Today* **2008**, *13*, 440. (c) Zaworotko, M.; Arora, K. Pharmaceutical co-crystals: A new opportunity in pharmaceutical science for a long-known but little studied class of compounds. In *Polymorphism in Pharmaceutical Solids*, 2nd ed.; Brittain, H. G., Ed.; Informa Healthcare: London, 2009.
(15) Lipinski, C. A. *J. Pharmacol. Toxicol.* **2000**, *44*, 235.
(16) Stanton, M. K.; Bak, A. *Cryst. Growth Des.* **2008**, *8*, 3856.
(17) Bak, A.; Gore, A.; Yanez, E.; Stanton, M.; Tufekcic, S.; Syed, R.; Akrami, A.; Rose, M.; Surapaneni, S.; Bostick, T.; King, A.; Neervannan, S.; Ostovic, D.; Koparkar, A. *J. Pharm. Sci.* **2008**, *97*, 3942.
(18) McNamara, D. P.; Childs, S. L.; Giordano, J.; Iarriccio, A.; Cassidy, J.; Shet, M. S.; Mannion, R.; O'Donnell, E.; Park, A. *Pharm. Res.* **2006**, *23*, 1888.
(19) (a) Chen, A. M.; Ellison, M. E.; Peresypkin, A.; Wenslow, R. M.; Variankaval, N.; Savarin, C. G.; Natishan, T. K.; Mathre, D. J.; Dormer, P. G.; Euler, D. H.; Ball, R. G.; Ye, Z. X.; Wang, Y. L.; Santos, I. *Chem. Commun.* **2007**, 419; E. (b) Dova; E. Mazurek, J. M.; Anker, J. Tenofovir disoproxil hemi-fumaric acid co-crystal. WO/2008/143500, **2008**; (c) Hickey, M. B.; Peterson, M. L.; Scoppettuolo, L. A.; Morrisette, S. L.; Vetter, A.; Guzman, H.; Remenar, J. F.; Zhang, Z.; Tawa, M. D.; Haley, S.; Zaworotko, M. J.; Almarsson, Ö. *Eur. J. Pharm. Biopharm.* **2007**, *67*, 112. (d) Imamura, M. Cocrystal of C-glycoside derivative and L-proline. WO 2007/114475 A1, **2007**. (e) Peterson, M.; Bourghol Hickey, M.; Oliveira, M.; Almarsson, Ö.; Remenar, J. Modafinil compositions. US 2005267209 A1, **2005**; (f) Remenar, J.; MacPhee, M.; Peterson, M.; Morissette, S. L.; Almarsson, Ö. Novel crystalline forms of conazoles and methods of making and using the same, WO/2005/092884, **2005**.
(20) Reutzel-Edens, S. M.; Bush, J. K.; Magee, P. A.; Stephenson, G. A.; Byrn, S. R. *Cryst. Growth Des.* **2003**, *3*, 897.
(21) Khankari, R. K.; Grant, D. J. W. *Thermochim. Acta* **1995**, *248*, 61.
(22) (a) Hickey, M. B.; Peterson, M. L.; Manas, E. S.; Alvarez, J.; Haeffner, F.; Almarsson, Ö. *J. Pharm. Sci.* **2007**, *96*, 1090. (b) Kobayashi, Y.; Ito, S.; Itai, S.; Yamamoto, K. *Int. J. Pharm.* **2000**, *193*, 137. (c) Salole, E. G.; Alsarraj, F. A. *Drug Dev. Ind. Pharm.* **1985**, *11*, 855. (d) Pudipeddi, M.; Serajuddin, A. T. M. *J. Pharm. Sci.* **2005**, *94*, 929.
(23) (a) Bowden, C. L. *Expert Opin. Pharmacol.* **2002**, *3*, 1513. (b) Goa, K. L.; Ross, S. R.; Chrisp, P. *Drugs* **1993**, *46*, 152.
(24) Motte, J.; Trevathan, E.; Arvidsson, J. F. V.; Barrera, M. N.; Mullens, E. L.; Manasco, P.; Dulac, O.; Mai, J.; Billard, C.; Vallee, L.; Oberarztin, F.; Ried, S.; Christe, W.; Rating, D.; Vigevano, F.; Tassinari, C.; Bernardina, B. D.; Majoie, H.; Weber, A.; Laegreid, L.; EegOlofsson, O.; Bermejo, M.; Martinez, A.; Castello, J. C.; Serra, M. T. I.; Kirkham, F.; Noronha, M.; Wallace, S.; Black, A.; Berkovic, S.; Pedespan, J.; Echenne, B.; Pinsard, N.; Parain, D.;

Peniello, M.; Carriere, J.; Chauvel, P.; Berquin, P.; Garrel, S.; Schaff, J.; Talvik, T.; Douchowny, M.; Gilman, J.; Pellock, J.; Cheng, R.; Crumrine, P.; Lynch, B.; Hahn, J.; Griesemer, D.; Wannamaker, B.; Laxer, K.; Bluestone, D.; Bebin, E. *New Engl. J. Med.* **1997**, *337*, 1807.
(25) Smith, D.; Baker, G.; Davies, G.; Dewey, M.; Chadwick, D. W. *Epilepsia* **1993**, *34*, 312.
(26) Sporn, J.; Sachs, G. *J. Clin. Psychopharm.* **1997**, *17*, 185.
(27) O'Neil, M. J. *Merck Index*, 14th ed.; Merck Research Laboratories: Whitehouse Station, NJ, 2006.
(28) (a) Floyd, A. G.; Jain, S. *Pharmaceutical composition containing lamotrigine*. U.S. Patent 5,942,510, **1999**; (b) Garti, N.; Berkovich, Y.; Dolitzky, B.-Z.; Aronhime, J.; Singer, C.; Liebermann, A.; Gershon, N. Crystal forms of lamotrigine and proecesses for their preparations. U.S. Patent 6,861,426 B2, **2005**; (c) Lee, G. R. Process for the preparation of lamotrigine. U.S. Patent 5,925,755, **1999**; (d) Parthasaradhi, R. B.; Rathnakar, R. K.; Raji, R. R.; Muralidhara, R. D.; Chander, R. K. S. Novel crystalline forms of lamotrigine. U.S. Patent 2005/0119265 A1, **2005**; (e) Winter, R. G.; Sawyer, D. A.; Germain, A. *Process for the preparation of lamotrigine*, U.S. Patent 5,912,345, **1999**.
(29) Aronhime, J.; Samburski, G. Pharmaceutical composition containing lamotrigine particles of defined morphology. U.S. Patent 2005/0238724 A1, **2005**.
(30) Galcera, J.; Molins, E. *Cryst. Growth Des.* **2009**, *9*, 327.
(31) Sridhar, B.; Ravikumar, K. *Acta Crystallogr. E* **2005**, *61*, o3805.
(32) Sridhar, B.; Ravikumar, K. *Mol. Cryst. Liq. Cryst.* **2007**, *461*, 131.
(33) Janes, R. W.; Lisgarten, J. N.; Palmer, R. A. *Acta Crystallogr. C* **1989**, *45*, 129.
(34) Sawyer, D. A.; Copp, F. C. *Triazine salt*. U.S. Patent 4,847,249, **1989**.
(35) Sridhar, B.; Ravikumar, K. *Acta Crystallogr. E* **2006**, *62*, O4752.
(36) Palmer, R.; Potter, B.; Leach, M.; Chowdhry, B. *J. Chem. Crystallogr.* **2007**, *37*, 771.
(37) Kubicki, M.; Codding, P. W. *J. Mol. Struct.* **2001**, *570*, 53.
(38) (a) Desiraju, G. R. *Angew. Chem., Int. Ed.* **1995**, *34*, 2311. (b) Bis, J. A.; Vishweshwar, P.; Weyna, D.; Zaworotko, M. J. *Mol. Pharmaceutics* **2007**, *4*, 401. (c) Shattock, T. R.; Arora, K. K.; Vishweshwar, P.; Zaworotko, M. J. *Cryst. Growth Des.* **2008**, *8*, 4533. (d) Shan, N.; Batchelor, E.; Jones, W. *Tetrahedron Lett.* **2002**, *43*, 8721. (e) Shan, N.; Bond, A. D.; Jones, W. *Cryst. Eng.* **2002**, *5*, 9. (f) Shan, N.; Bond, A. D.; Jones, W. *Tetrahedron Lett.* **2002**, *43*, 3101. (g) Shan, N.; Jones, W. *Tetrahedron Lett.* **2003**, *44*, 3687.
(39) Weyna, D. R.; Shattock, T.; Vishweshwar, P.; Zaworotko, M. J. *Cryst. Growth Des.* **2009**, *9*, 1106.
(40) Allen, F. H. *Acta Crystallogr. B* **2002**, *58*, 380.
(41) CSD November 2007 release including August 2008 update. Search parameters: organics only, no ions, 3D coordinates determined, $R < 7.5\%$
(42) (a) Friščić, T.; Jones, W. *Cryst. Growth Des.* **2009**, *9*, 1621. (b) Etter, M. C.; Reutzel, S. M.; Choo, C. G. *J. Am. Chem. Soc.* **1993**, *115*, 4411. (c) Shan, N.; Jones, W. *Green Chem.* **2003**, *5*, 728.
(43) *SMART, SAINT-Plus, SADABS, XP and SHELXTL*; Bruker: Madison, Wisconsin, USA, 1997.
(44) Sheldrick, G. M. *SHELXTL*; University of Gottingen: Germany, 1997.
(45) It is noted that this dissolution study did not use the standard USP apparatus, due to the limitations of our in-house facility. Nevertheless, it is believed that our dissolution study produced reasonably comparable results. As part of the future development, a dissolution study through a contract research organization using the standard USP apparatus will be conducted.
(46) Castel-Branco, M. M.; Almeida, A. M.; Falcao, A. C.; Macedo, T. A.; Caramona, M. M.; Lopez, F. G. *J. Chromatogr. B* **2001**, *755*, 119.
(47) Delori, A.; Suresh, E.; Pedireddi, V. R. *Chem.−Eur. J.* **2008**, *14*, 6967. Bhogala, B. R.; Basavoju, S.; Nangia, A. *CrystEngComm* **2005**, *7*, 551.
(48) Childs, S. L.; Stahly, G. P.; Park, A. *Mol. Pharmaceutics* **2007**, *4*, 323.
(49) (a) Cabelli, D. E.; Bielski, B. H. J. *Z. Naturforschung B* **1985**, *40*, 1731. (b) Gavrilov, A. V.; Kurmaeva, A. I.; Barabonov, V. P. *Russ. J. Phys. Chem.* **1980**, *54*, 902. (c) Koppel, I.; Koppel, J.; Leito, I.; Pihl, V.; Grahn, L.; Ragnarsson, U. *J. Chem. Res., Miniprint* **1994**, *6*, 1173. (d) Orekhova, Z.; Ben-Hamo, M.; Manzurola, E.; Apelblat, A. *J. Solution Chem.* **2005**, *34*, 687.
(50) Potter, B.; Palmer, R. A.; Withnall, R.; Leach, M. J.; Chowdhry, B. Z. *J. Chem. Cryst.* **1999**, *29*, 701.
(51) Boenigk, D.; Mootz, D. *J. Am. Chem. Soc.* **1988**, *110*, 2135.
(52) Banerjee, R.; Bhatt, P. M.; Ravindra, N. V.; Desiraju, G. R. *Cryst. Growth Des.* **2005**, *5*, 2299.
(53) Rodríguez-Hornedo, N.; Lechuga-Ballesteros, D.; Hsiu-Jean, W. *Int. J. Pharm.* **1992**, *85*, 149.
(54) Childs, S. L.; Chyall, L. J.; Dunlap, J. T.; Smolenskaya, V. N.; Stahly, B. C.; Stahly, G. P. *J. Am. Chem. Soc.* **2004**, *126*, 13335.
(55) Good, D. J.; Rodríguez-Hornedo, N. *Cryst. Growth Des.* **2009**, *9*, 2252.
(56) Rasool, A. A.; Hussain, A. A.; Ditter, L. W. *J. Pharm. Sci.* **1991**, *80*, 387.